Equivalent Mass-Spring Models of Multibody Spacecraft for the Application of Wave-based Control

Joseph W. Thompson

School of Mechanical and Materials Engineering
University College Dublin
Belfield, Dublin 4, Ireland
joseph.thompson@ucdconnect.ie

Abstract

Wave-Based Control (WBC) is particularly effective for achieving rest to rest motion of under-actuated, cascaded, lumped flexible systems. In this control scheme the actuator simultaneously launches and absorbs wave components travelling into and out of the system at one end. By doing this the control scheme combines position control and active vibration damping. Much work has been done on wave-based modelling and control of mass-spring strings. This paper asks the question: to what extent can this work be extended to a wider class of systems? This question is motivated by the control of spacecraft with features such as structural flexibility, flexible appendages and fuel slosh. Most mathematical models of these systems presented to the control engineer, do not obviously have the structure of a mass-spring string. However, often it is possible to calculate an equivalent mass-spring system. This paper identifies a class of systems, with real, positive and distinct eigenvalues, for which this transformation is possible and presents an algorithm for calculating the equivalent mass and spring values. A segmented planar multibody rocket model is used as an example. This model consists of three rigid bodies connected by two torsional springs. The rocket has several lateral thrusters and a gimballed rocket engine which may be used for attitude control. Several test cases with different sensor and actuator configurations are examined. Equivalent mass-spring systems are calculated in each case. Wave-based controllers are designed and tested for each model.

Keywords: Spacecraft Dynamics, Attitude Control, Flexible Systems, Sloshing, Mechanical Waves

1. Introduction

Many spacecraft and rockets may be modelled as multi-body systems [1, 3, 10]. Flexible structures, such as solar panel arrays and robot arms, may be approximated by lumped equivalents: a number of rigid bodies, with inter-connecting springs. Sloshing fuel may be represented by a simple pendulum or mass-spring analog. These simple representations are particularly useful in the design of attitude controllers. Such systems are usually under-actuated, i.e. have more degrees of freedom than actuators. In attempting to re-orient such a system, one will usually excite certain modes of vibration. In bringing the system back to rest, the control algorithm must effectively dampen these vibrations while imposing the desired motion.

To end up at rest with the correct target attitude at the end of a manoeuvre the excitation and subsequent damping of vibrations must be done in precisely the right way. One approach which facilitates this is to model the motion of each part of the system as a superposition of two component motions or 'waves'. Using this wave-based interpretation of the system, linear controllers have been designed with a number of desirable properties. These include robustness to modelling errors, to system changes, to sensor delays and to non-ideal actuation, while requiring minimal sensing and being easy to implement. This so-called "wave-based control" (WBC) has been applied successfully to uniform and non-uniform in-line mass-spring systems [4, 5, 6, 7, 8]. The aim of this paper is to extend the WBC theory to a wider class of systems, and in particular the multi-body spacecraft described above.
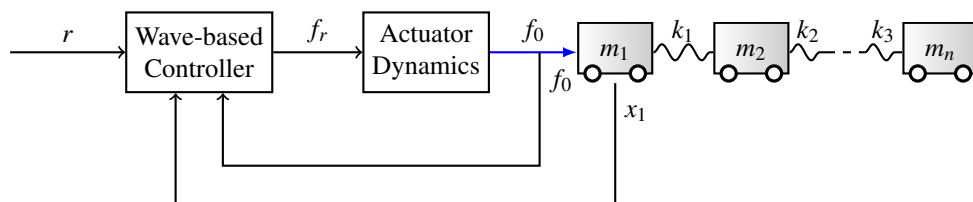

Figure 1: Wave-based control scheme for a mass-spring string

Fig. 1 shows a simple WBC control system. The generic in-line (cascaded) mass-spring system shown is a classical example of an under-actuated control problem. The motion of this lumped system may be modelled as a superposition of two "waves" or wave-like components travelling rightwards and leftwards, with more or less dispersion as they go. One wave is travelling from the actuator into and through the system, rightwards, and the other is travelling leftwards through the system, back towards the actuator. In this way the actuator is simultaneously launching a wave into the system and absorbing a returning wave from the system. The returning wave is a delayed and dispersed version of the initial launched wave. A complete manoeuvre consists of launching a specified wave into the system, allowing it to travel towards the boundary of the system (right-hand end) where it is reflected, and the motion (returning wave) travels leftwards back to the actuator, which moves to absorb it and bring the system back to rest, leaving behind a net displacement of the system equal to the target displacement. This returning wave is resolved using two measurements from the system. These measurements can be positions, velocities or forces and are usually taken close to the actuator.

In Fig. 1 these measurements are the position of the first mass x_1 and the force being applied to the first mass f_0. In addition to the cascaded mass-spring system shown in Fig. 1 this type of controller has also been applied to a much wider variety of systems, including 2-D arrays of masses and springs and 3-D multibody systems. However in these more complex cases the approach to controller design and tuning, while wave-inspired, has been experimental in nature. The underlying notional waves were not clearly defined. It is proposed here that many of these more complex systems can be considered in fact to be similar in dynamical structure to the mass-spring system in Fig. 1. Furthermore it is proposed that through a suitable change of coordinates, an equivalent in-line mass-spring system may be calculated for many of these systems.

Such a transformation provides a better theoretical foundation for applying wave-based modelling and control design to systems which, at first sight, are quite different from the cascaded masses and springs for which wave behavior is better understood and measured. In addition, the parameters and configuration of the transformed system provide strong insights into the control challenge in the original system, and throws light on how the location of actuators and sensors affects the control.

Problem Statement

The problem can be stated as follows. Given a SISO (single-input single-output) undamped system described by:

$$\ddot{\mathbf{q}}(t) + \Lambda \mathbf{q}(t) = \mathbf{b}u(t) \tag{1}$$

$$y(t) = \mathbf{c}^T \mathbf{q}(t) \tag{2}$$

where

$$\Lambda = \begin{bmatrix} \lambda_1 & 0 & \cdots & 0 \\ 0 & \lambda_2 & \ddots & 0 \\ \vdots & \ddots & \ddots & \vdots \\ 0 & 0 & \cdots & \lambda_n \end{bmatrix}, \quad \mathbf{b} = \begin{bmatrix} b_1 \\ b_2 \\ \vdots \\ b_n \end{bmatrix}, \quad \mathbf{c} = \begin{bmatrix} c_1 \\ c_2 \\ \vdots \\ c_n \end{bmatrix} \tag{3}$$

where $u(t)$ is the input and $y(t)$ is the output,

1. under what conditions can this system be transformed into an equivalent mass-spring string such as in Fig.1 (for which WBC is known to work well) and

2. how can the parameters of this equivalent system be calculated?

Alternatively we ask if there exists a coordinate transformation from $\mathbf{q}$ to a new coordinate system $\mathbf{x}$,

$$\mathbf{x} = P\mathbf{q} \tag{4}$$

such that:

$$M\ddot{\mathbf{x}}(t) + K\mathbf{x}(t) = \hat{\mathbf{b}}u(t) \tag{5}$$

$$y(t) = \hat{\mathbf{c}}^T \mathbf{x}(t) \tag{6}$$

where M, K, $\hat{\mathbf{b}}$ and $\hat{\mathbf{c}}$ have the following structure:

$$M = \begin{bmatrix} m_1 & 0 & \cdots & 0 \\ 0 & m_2 & \ddots & 0 \\ \vdots & \ddots & \ddots & \vdots \\ 0 & 0 & \cdots & m_n \end{bmatrix}, \quad K = \begin{bmatrix} k_0 + k_1 & -k_1 & 0 & \cdots & 0 \\ -k_1 & k_1 + k_2 & -k_2 & \ddots & 0 \\ 0 & -k_2 & \ddots & \ddots & \vdots \\ \vdots & & \ddots & k_{n-1} + k_{n-2} & -k_{n-1} \\ 0 & 0 & \cdots & -k_{n-1} & k_{n-1} + k_n \end{bmatrix}, \quad \hat{\mathbf{b}} = \begin{bmatrix} 1 \\ 0 \\ \vdots \\ 0 \end{bmatrix}, \quad \hat{\mathbf{c}} = \begin{bmatrix} 1 \\ 0 \\ \vdots \\ 0 \end{bmatrix} \tag{7}$$

Section 2 answers in the affirmative and presents a procedure for calculating the transformation P of Eq. 4. The problem may first be reduced to an inverse eigenvalue problem for a Jacobi matrix. This is then solved using the Lanczos algorithm. Finally mass and stiffness matrices are reconstructed. It is found that there are some necessary conditions for the transformation to be possible. Section 3 presents a mathematical model of a multibody flexible rocket which will be used as an example to test the algorithms presented in Section 2. Linearised equations of motion are presented for the system. Section 4 presents some numerical examples of transformations for the rocket model. Numerical parameters are chosen for the model to represent the European rocket *Vega*. It is found that there are many equivalent mass-spring systems depending on the locations of actuators and sensors on the rocket and some different examples are considered. Sections 5 and 6 present discussion and conclusions respectively.

2. Equivalent Mass-Spring Models

This section outlines a procedure for converting a generic SISO vibrating system described by Eqs. 1-3 to an in-line mass-spring system described by Eqs. 5-7. This conversion amounts to finding the transformation matrix P of Eq. 4. The coordinate transformation is carried out in three steps.

2.1. Scaling the States of the System

First consider the transformation $\mathbf{v} = A\mathbf{q}$ where $A = diag(a_1, a_2, ..., a_n)$ is a diagonal matrix with strictly positive diagonal. This transformation merely scales the states of the system and leads to the new system:

$$\ddot{\mathbf{v}}(t) + \Lambda\mathbf{v}(t) = A^{-1}\mathbf{b}u(t) \tag{8}$$

$$y(t) = \mathbf{c}^T A\mathbf{v}(t) \tag{9}$$

Here the input and output vectors $\mathbf{b}$ and $\mathbf{c}$ are changed. Note however the matrix Λ of eigenvalues is unaffected by the transformation. The choice of values a_i are used to achieve the correct form of the input and output $\hat{\mathbf{b}}$ and $\hat{\mathbf{c}}$ vectors of the mass-spring system after the final step. The values of the a_i are calculated in Section 2.3 below.

2.2. Inverse Eigenvalue Problem for Jacobi Matrix and Lanczos Algorithm

Gladwell [2] investigates inverse eigenvalue problems for Jacobi matrices which are defined as follows: a Jacobi matrix is a positive semi-definite symmetric tri-diagonal matrix with strictly negative co-diagonal. We make use of the following theorem for Jacobi matrices:

There is a unique Jacobi matrix $\mathbf{J}$ having specified eigenvalues $(\lambda_i)_1^n$, where

$$0 \leq \lambda_1 < \lambda_2 < \cdots < \lambda_n \tag{10}$$

and with normalised eigenvectors $(\mathbf{u}_i)_1^n$ having non-zero specified values $(u_{1i})_1^n$ of their first components. Recall that $\mathbf{u}_i = \begin{bmatrix} u_{1i} & u_{2i} & \cdots & u_{ni} \end{bmatrix}^T$.

To simplify notation let U be the orthogonal matrix whose columns are the eigenvectors $\mathbf{u}_i$ of the Jacobi matrix J and let X be the transpose of U with columns $\mathbf{x}_i$. Then the theorem says that for a given Λ and $\mathbf{x_1}$ (the first column of X) there is a unique Jacobi matrix J and orthogonal matrix U. The Lanczos algorithm may be used to calculate the matrices J and U (X^T) for a given Λ and $\mathbf{x_1}$ such that

$$JU = U\Lambda \tag{11}$$

This may be rewritten in terms of X as

$$XJ = \Lambda X \tag{12}$$

The Lanczos algorithm works as follows. Eq. 12 may be expanded as

$$\begin{bmatrix} \mathbf{x_1} & \mathbf{x_2} & \cdots & \mathbf{x_n} \end{bmatrix} \begin{bmatrix} d_1 & -e_1 & 0 & \cdots & 0 \\ -e_1 & d_2 & -e_2 & \ddots & 0 \\ 0 & -e_2 & \ddots & \ddots & \vdots \\ \vdots & \ddots & \ddots & d_{n-1} & -e_{n-1} \\ 0 & 0 & \cdots & -e_{n-1} & d_n \end{bmatrix} = \Lambda \begin{bmatrix} \mathbf{x_1} & \mathbf{x_2} & \cdots & \mathbf{x_n} \end{bmatrix} \tag{13}$$

Taking this column by column, first we have

$$d_1\mathbf{x_1} - e_1\mathbf{x_2} = \Lambda\mathbf{x_1} \tag{14}$$

If we pre-multiply by $\mathbf{x_1^T}$, using $\mathbf{x_1^T x_1} = 1$ and $\mathbf{x_1^T x_2} = 0$ we get

$$d_1 = \mathbf{x_1^T} \Lambda \mathbf{x_1} \tag{15}$$

Then rewriting Eq. 14 as

$$e_1 \mathbf{x_2} = d_1 \mathbf{x_1} - \Lambda \mathbf{x_1} = \hat{\mathbf{x}}_2 \tag{16}$$

The vector $\hat{\mathbf{x}}_2$ is may be calculated from d_1, $\mathbf{x_1}$ and Λ and since $\mathbf{x_2}$ is a unit vector e_1 may be calculated from

$$e_1 = \|\hat{\mathbf{x}}_2\| \tag{17}$$

and then

$$\mathbf{x_2} = \frac{\hat{\mathbf{x}}_2}{e_1} \tag{18}$$

This procedure of Eqs. 14 to 18 may be repeated for each column of the equation calculating all the d_i, e_i and $\mathbf{x_i}$.

Using this algorithm we can find the second transformation $\mathbf{z} = U\mathbf{v}$ which leads to the new system:

$$\ddot{\mathbf{z}}(t) + J\mathbf{z}(t) = UA^{-1}\mathbf{b}u(t) \tag{19}$$

$$y(t) = \mathbf{c}^T AU^T \mathbf{z}(t) \tag{20}$$

Note that this transformation is only possible if Eq. 10 holds.

2.3. Reconstruction of Mass and Stiffness Matrices

The final step is to reconstruct the mass and stiffness matrices M and K. It can be shown that $J = M^{-\frac{1}{2}}KM^{-\frac{1}{2}}$ and the transformation $\mathbf{x} = M^{\frac{1}{2}}\mathbf{z}$ where M has the form given in Eq. 7 leads to the final system:

$$M\ddot{\mathbf{x}}(t) + K\mathbf{x}(t) = M^{\frac{1}{2}}UA^{-1}\mathbf{b}u(t) \tag{21}$$

$$y(t) = \mathbf{c}^T AU^T M^{\frac{1}{2}}\mathbf{x}(t) \tag{22}$$

The matrix M is calculated as follows: We can write $K = M^{\frac{1}{2}}JM^{\frac{1}{2}}$ where K and M are mass and stiffness matrices of Eq. 7 which we want to calculate. We will only consider here the case where $k_0 = k_n = 0$ and where K (and J) are singular, corresponding to a free-free mass-spring system. In this case one eigenvalue of the system $\lambda_1 = 0$. The example we show later in the paper is indeed such a system. The rows of K must sum to zero. This can be written as

$$K \begin{bmatrix} 1 & 1 & \cdots & 1 \end{bmatrix}^T = M^{\frac{1}{2}}JM^{\frac{1}{2}} \begin{bmatrix} 1 & 1 & \cdots & 1 \end{bmatrix}^T = \mathbf{0} \tag{23}$$

which may be rewritten as

$$J \begin{bmatrix} \sqrt{m_1} & \sqrt{m_2} & \cdots & \sqrt{m_n} \end{bmatrix}^T = \mathbf{0} \tag{24}$$

Once a value is chosen for m_1 this equation may be solved row by row to calculate each m_i. The values of the k_i easily follow. The correct choice for m_1 is shown in Eq. 28 below.

By comparing this system to that of Eqs. 5-7 we get the following equation for $\mathbf{b}$ and $\mathbf{c}$.

$$M^{\frac{1}{2}}UA^{-1}\mathbf{b} = M^{\frac{1}{2}}UA\mathbf{c} = \begin{bmatrix} 1 & 0 & \cdots & 0 \end{bmatrix}^T \tag{25}$$

which can be simplified to

$$A^{-1}\mathbf{b} = A\mathbf{c} = \frac{1}{m_1}U^T \begin{bmatrix} 1 & 0 & \cdots & 0 \end{bmatrix}^T \tag{26}$$

and then

$$A^{-1}\mathbf{b} = A\mathbf{c} = \frac{1}{m_1}\mathbf{x_1} \tag{27}$$

This can be solved to give

$$a_i = \sqrt{\frac{b_i}{c_i}}, \quad m_1 = \sqrt{\frac{1}{\sum b_i c_i}}, \quad x_{i1} = \sqrt{\frac{b_i c_i}{\sum b_i c_i}} \tag{28}$$

By combining the three steps the overall transformation can be written as

$$P = M^{-\frac{1}{2}}UA^{-1} \tag{29}$$

Examining Eq. 28 we find that a second necessary and sufficient condition for P to exist is

$$\frac{b_i}{c_i} > 0 \quad \forall i \tag{30}$$

that is, the sign of each b_i term is the same as the corresponding c_i term. Also note however that if

$$\frac{b_i}{c_i} < 0 \quad \forall i \tag{31}$$

then we can write down a new system by changing the signs of both $u(t)$ and $\mathbf{b}$. We then have a new system identical to the old system but where the input is $-u(t)$ and Eq. 30 is satisfied. This condition may be summarized as: the corresponding entries in the $\mathbf{b}$ and $\mathbf{c}$ vectors must either all have the same sign or all have opposite signs.

3. Mathematical Model of Segmented Rocket

In this section the equations of motion for a planar segmented model of a rocket are presented. At first sight it might appear that this lumped model, comprising three bodies and two springs, is just like a cascaded mass-spring system of three masses and two springs. Dynamically however it is quite different. The subtle but important differences, which will become clearer in subsequent sections, are what motivate the current study. From a control perspective the system inputs and the measured outputs are key. In the mass-spring system of Fig. 1 the input and measured output are the force on the first mass and the position of the first mass respectively. This is the preferred arrangement to apply wave-based control. When the input is a gimballed engine acting on the lowest segment and the measured output is the angle of this lowest segment, then it will be shown that the system is indeed similar to a cascaded 3-mass, 2-spring system. However, even if the segments in the rocket model have equal masses and moments of inertia, the corresponding equivalent mass-spring system is not uniform. Furthermor the correct choices for the equivalent masses and springs are far from obvious. We might distinguish between outputs which are measured and used for control, and possible other system outputs, such as the orientation of the tip. In the present examples, however, where the reference and measured variables are angles (or attitude), the distinction does not matter, because if the control system succeeds in damping the vibrations, then the final angles of all segments will be equal.
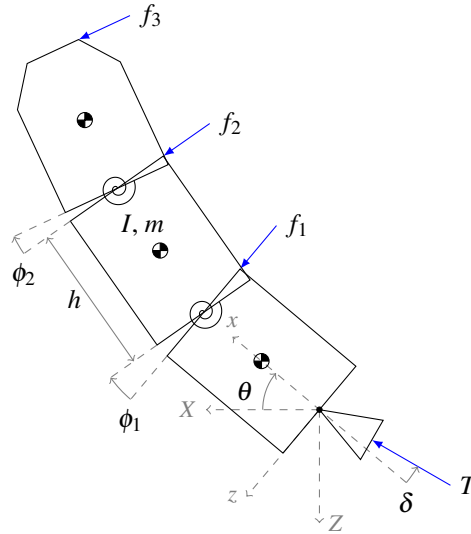

Figure 2: Segmented planar rocket model

The model, shown in Fig. 2, consists of three rigid bodies connected by two torsional springs as shown in Fig. 2. The attitude of the bottom or base segment is θ relative to an inertial reference frame. The middle and top segments have angles ϕ_1 and ϕ_2 respectively between themselves and the segment below as shown. Each segment has has height h, mass m and moment of inertia I about its mass centre and each torsional spring has stiffness k. The rocket is considered to have four possible sources of actuation: three lateral thruster forces f_i at the top of each segment and an engine that may be gimballed by angle δ on the bottom segment as shown. This combination of inputs allow many different cases to be considered. Similarly the rocket has three outputs or attitude sensors, one on each segment which we will call α_1, α_2 and α_3 respectively The rotational equations of motion of the system were derived using Kane's method [3]

and linearised about the equilibrium point $\theta = \dot{\theta} = \phi_i = \dot{\phi}_i = 0$. Aerodynamic effects are here ignored, to simplify the illustration of the general idea, implicitly restricting the applicability to manoeuvres beyond the atmosphere.

$$
\begin{bmatrix} 3I+2h^2m & 2I+\frac{3m}{2}h^2 & I+\frac{h^2m}{2} \\ 2I+\frac{3m}{2}h^2 & 2I+\frac{7m}{6}h^2 & I+\frac{5m}{12}h^2 \\ I+\frac{h^2m}{2} & I+\frac{5m}{12}h^2 & I+\frac{h^2m}{6} \end{bmatrix} \begin{bmatrix} \ddot{\theta} \\ \ddot{\phi}_1 \\ \ddot{\phi}_2 \end{bmatrix}
$$

$$
+ \begin{bmatrix} 0 & -\frac{2T}{3}h & -\frac{Th}{6} \\ 0 & -\frac{2T}{3}h+k & -\frac{Th}{6} \\ 0 & -\frac{Th}{6} & -\frac{Th}{6}+k \end{bmatrix} \begin{bmatrix} \theta \\ \phi_1 \\ \phi_2 \end{bmatrix} = \begin{bmatrix} \frac{3T}{2}h & \frac{h}{2} & -\frac{h}{2} & -\frac{3h}{2} \\ \frac{2T}{3}h & \frac{2h}{3} & -\frac{h}{3} & -\frac{4h}{3} \\ \frac{Th}{6} & \frac{h}{6} & \frac{h}{6} & -\frac{5h}{6} \end{bmatrix} \begin{bmatrix} \delta \\ f_1 \\ f_2 \\ f_3 \end{bmatrix} \tag{32}
$$

$$
\begin{bmatrix} \alpha_1 \\ \alpha_2 \\ \alpha_3 \end{bmatrix} = \begin{bmatrix} 1 & 0 & 0 \\ 1 & 1 & 0 \\ 1 & 1 & 1 \end{bmatrix} \begin{bmatrix} \theta \\ \phi_1 \\ \phi_2 \end{bmatrix} \tag{33}
$$

4. Examples

Table 1: Summary of model parameters representative of *Vega* rocket

Parameter	Value	Unit
m	$5 \cdot 10^4$	kg
k	$6 \cdot 10^7$	Nm
I	$5 \cdot 10^5$	$kg\ m^2$
h	10	m
T	$2.3 \cdot 10^6$	N

Tab. 1 presents numerical parameters for the model presented in Section 3 which are representative of the European launcher *Vega* [9]. These values were substituted into the rocket equations of motion and then the system was diagonalised to have the same structure as Eqs. 1 to 3.

$$
\begin{bmatrix} \ddot{q}_1 \\ \ddot{q}_2 \\ \ddot{q}_3 \end{bmatrix} + \begin{bmatrix} 0 & 0 & 0 \\ 0 & 61.3 & 0 \\ 0 & 0 & 309.0 \end{bmatrix} \begin{bmatrix} q_1 \\ q_2 \\ q_3 \end{bmatrix} = \begin{bmatrix} 2.73 & 5.08 \cdot 10^{-7} & -4.08 \cdot 10^{-7} & -1.39 \cdot 10^{-6} \\ -14.7 & 3.19 \cdot 10^{-6} & 3.19 \cdot 10^{-6} & -6.38 \cdot 10^{-6} \\ 19.9 & -1.05 \cdot 10^{-5} & 1.06 \cdot 10^{-5} & -8.93 \cdot 10^{-6} \end{bmatrix} \begin{bmatrix} \delta \\ f_1 \\ f_2 \\ f_3 \end{bmatrix} \tag{34}
$$

$$
\begin{bmatrix} \alpha_1 \\ \alpha_2 \\ \alpha_3 \end{bmatrix} = \begin{bmatrix} 1.0 & -0.592 & 0.322 \\ 1.0 & -0.00814 & -0.347 \\ 1.0 & 0.547 & 0.322 \end{bmatrix} \begin{bmatrix} q_1 \\ q_2 \\ q_3 \end{bmatrix} \tag{35}
$$

These equations actually represent twelve possible SISO systems using the four possible actuators (represented by the columns of **b**) and three possible sensors (represented by the rows of **c**). By examining the sign patterns of the input and output matrices, we find that there are only three combinations which satisfy the sign condition of Eq. 30. These are (δ, α_1), $(-f_2, \alpha_2)$ and $(-f_3, \alpha_3)$. Note that the input in the latter two cases are negative. The algorithms described in Section 2 were used to calculate the equivalent mass-spring system for each of these cases. Let $\mathbf{x} = \hat{P} \begin{bmatrix} \theta & \phi_1 & \phi_2 \end{bmatrix}^T$ be the coordinate transformation from the original rocket system to the mass-spring system. Then the matrix $\hat{P}$ for each case is:

$$
\hat{P}_{\delta,\alpha_1} = \begin{bmatrix} 1 & 0 & 0 \\ 1 & 0.740 & -0.315 \\ 1 & 0.933 & 0.502 \end{bmatrix}, \quad \hat{P}_{f_2,\alpha_2} = \begin{bmatrix} 1 & 1 & 0 \\ 1 & 0.720 & 0.298 \\ 1 & 0.901 & 0.406 \end{bmatrix}, \quad \hat{P}_{f_3,\alpha_3} = \begin{bmatrix} 1 & 1 & 1 \\ 1 & 1.302 & 0.257 \\ 1 & 0.489 & 0.065 \end{bmatrix} \tag{36}
$$

Fig. 3 shows these equivalent systems. Tab. 2 summarizes the equivalent mass and spring values.

4.1. WBC Step Responses

WBC controllers were designed for each of the three systems in Fig. 3. A comprehensive introduction to WBC is beyond the scope of this paper but the reader may refer to [4] for more information. The controller is a fourth order linear system and may be written in standard state space notation as:

$$
\dot{\mathbf{x}}_{\mathbf{w}}(t) = A_w \mathbf{x}_{\mathbf{w}}(t) + B_w \mathbf{u}_{\mathbf{w}}(t) \tag{37}
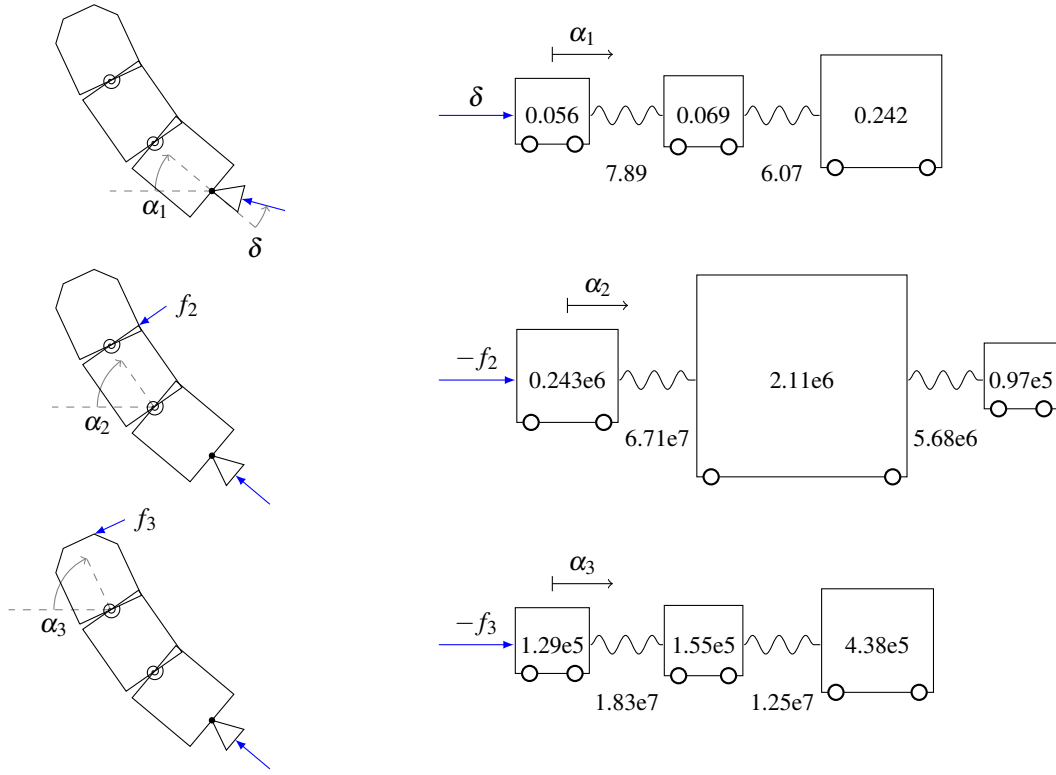$$

Figure 3: Equivalent mass-spring systems for three different actuator-sensor combinations

Table 2: Equivalent mass and spring values for three different actuator-sensor combinations

Input	Output	m_1	m_2	m_3	k_1	k_2
δ	α_1	0.056	0.069	0.242	7.89	6.07
$-f_2$	α_2	$0.243 \cdot 10^6$	$2.11 \cdot 10^6$	$0.0965 \cdot 10^6$	$6.71 \cdot 10^7$	$0.568 \cdot 10^7$
$-f_3$	α_3	$1.29 \cdot 10^5$	$1.55 \cdot 10^5$	$4.38 \cdot 10^5$	$1.83 \cdot 10^7$	$1.25 \cdot 10^7$

$$f_r(t) = C_w \mathbf{x_w}(t) + D_w \mathbf{u_w}(t) \tag{38}$$

$$A_w = \begin{bmatrix} 0 & 1 & 0 & 0 \\ -\omega^2 & -\omega & -\omega^2 & 0 \\ 0 & 0 & 0 & 1 \\ -\omega^2 & 0 & -\omega^2 & -\omega \end{bmatrix}, \quad B_w = \begin{bmatrix} 0 & 0 & 0 \\ 0 & \omega^2 & 0 \\ 0 & 0 & 0 \\ \frac{\omega^2}{k_0} & \omega^2 & 0 \end{bmatrix}, \quad C_w = \begin{bmatrix} k_0 & 0 & 0 & 0 \end{bmatrix}, \quad D_w = \begin{bmatrix} 0 & -k_0 & \frac{k_0}{2} \end{bmatrix} \tag{39}$$

The controller has three inputs as shown in Fig. 1, the position of the first mass x_1, the force applied to the first mass f_0 and the reference r.

$$\mathbf{u_w}(t) = \begin{bmatrix} x_1(t) & f_0(t) & r(t) \end{bmatrix}^T \tag{40}$$

The output is the requested force to the actuator f_r. In the simulations to follow the actuator is considered to be ideal so that $f_r = f_0$. The controller has two tuning parameters, ω and k_0. In each case these parameters are set to $\omega = \sqrt{\frac{k_1}{m_1}}$ and $k_0 = k_1$. These are the standard tuning choices for these parameters in the case of a mass-spring system. The step response for each closed loop system is shown in Fig. 4.
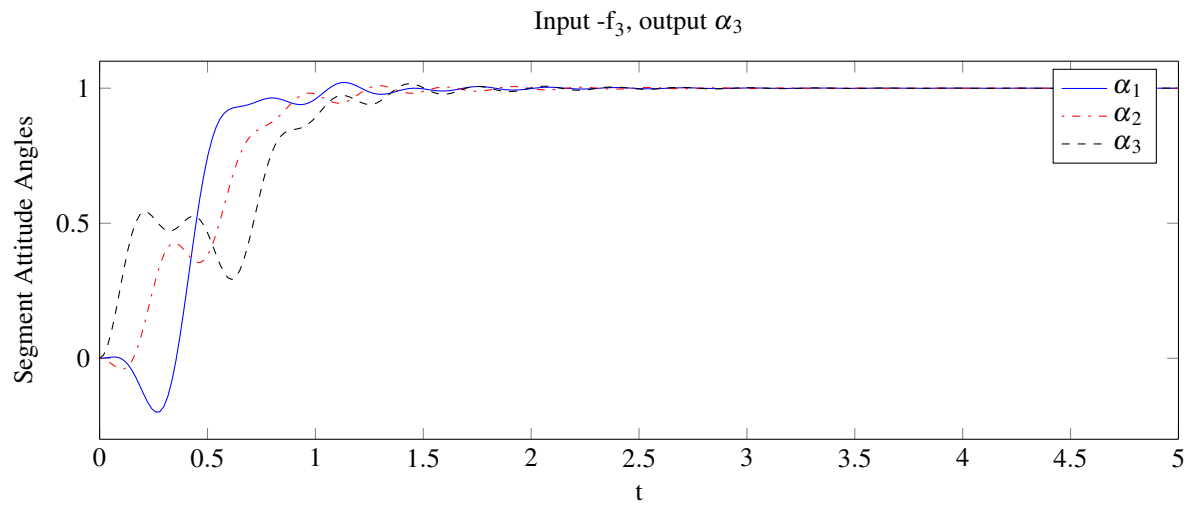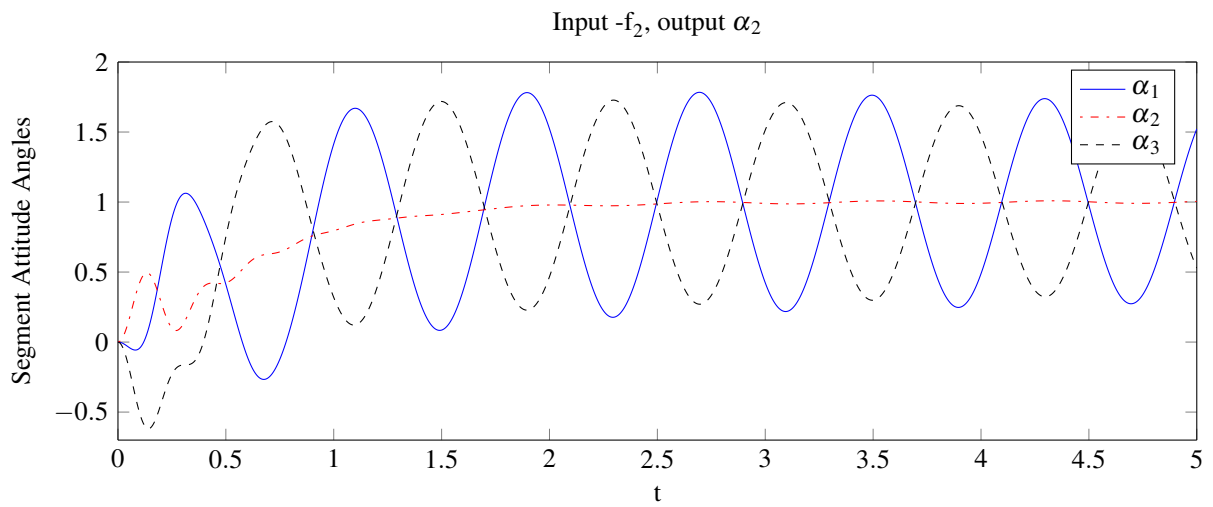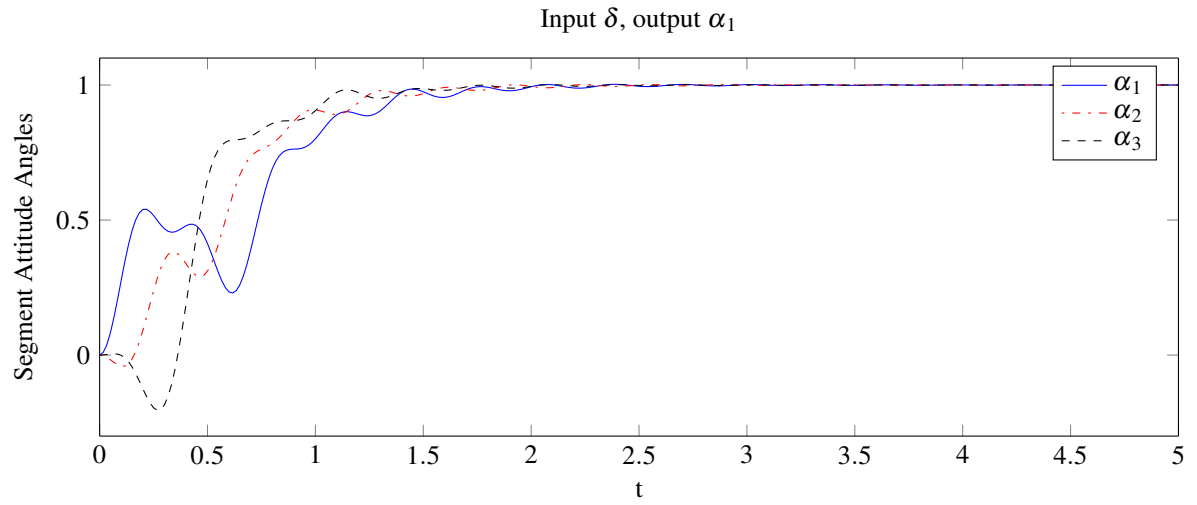
Figure 4: Step responses of a simple wave-based control system for each choice of actuator and sensor

5. Discussion

WBC was developed with reference to cascaded mass-spring systems such as that in Fig. 1. When designing a WBC controller for these systems the underlying wave model, which is well understood, naturally suggests the best tuning parameters for the controller. While the technique has also been applied successfully to systems with more complex structure such as bending and slewing systems, cranes and 2-D mass-spring arrays, in these cases tuning has been carried out somewhat experimentally without reference to the underlying wave model. This paper asserts that many of these more complicated systems have the same underlying structure as simple mass-spring cascades with actuator and sensor at one end. An algorithm is presented for calculating these equivalent mass-spring systems. Using these equivalent mass-spring representations allows us to quickly design and tune controllers for a much wider class of systems including multibody spacecraft models. In addition, previously established analytical results concerning stability and robustness of WBC for mass-spring systems are now readily applicable to this wider class of systems.

Given the choices of actuators and sensors for the rocket model presented in Sec. 3 we have found that there are three configurations which allow us to calculate an equivalent mass-spring system with both actuator and sensor at one end. The first system with actuator δ and sensor α_1 both on the bottom segment is somewhat expected and has obvious similarities to a 3-mass, 2-spring system. Interestingly, even though the rocket segments are identical, the ratio of the masses in the equivalent mass-spring system is [1:1.2:4.3] which is quite non-uniform with masses increasing as they get farther from the actuator and nearly equal springs. The system with actuator $-f_3$ and sensor α_3 is very similar with mass ratio [1:1.2:3.4] also increasing farther from the actuator and also with similar springs. There is an obvious symmetry between these two systems. One launches and absorbs waves at the bottom of the rocket and the other launches and absorbs at the top. When WBC is applied to these systems the step response of the closed-loop systems are seen to behave excellently with minimal overshoot and small settling times (Figs. 4(a), 4(c)). The final system with actuator $-f_2$ and sensor α_2 has a mass ratio of [1:8.7:0.4] and spring ratio of [1:0.08] which is highly non-uniform. In the step response for this system we can see that the measured variable α_2 approaches the target and settles quickly with small oscillations around the target attitude. However the other rocket segments continue to oscillate about the target for a long period of time.

The above phenomena can be explained from a wave perspective. A change in mass in a non-uniform system can be considered as a change in wave impedance causing partial transmission and reflection of waves. In the case where mass increases farther away from the actuator, some of the launched wave is reflected back at these changes in impedance. This is not a problem however as the actuator can launch a further wave to compensate and ensure the system reaches the target. Conversely, in the case where there is a large mass in the centre of the system (Fig. 4(b)), returning waves are reflected back into the farthest part of the system and become trapped by the larger mass in the centre. This is the reason for the prolonged oscillations in the system of Fig. 4(b). It should be noted that this poor response is not a failing of the WBC technique but rather an indication of the difficulty of the control problem. Any controller measuring at the first mass will have to somehow measure the motion of the smaller end mass through the large mass in the centre of the system. Then to control that end mass the actuator must work through the intervening dynamics of the large mass in between. It is clear form this analysis that the non-uniformity of the system plays a key role in assessing the difficulty of the control problem. It is the position of the non-uniformity, rather than the ratio of the masses or springs that is the key determining factor in the difficulty of the problem.

6. Conclusions

A procedure has been presented for calculating equivalent cascaded mass-spring representations of a wide class of SISO systems. In these equivalent mass-spring representations, the input is a force on the first mass and the output is the position of the first mass. These are the type of systems for which WBC has been shown to work well. The transformation is possible for a system described by Eqs. 1-3, with non-negative and distinct eigenvalues and corresponding entries in the **b** and **c** vectors either all having the same sign or all having opposite signs. The transformation may be formulated as an inverse eigenvalue problem for a Jacobi matrix and solved using the Lanczos algorithm. As an example, the equations of motion were derived for a segmented multibody rocket with twelve possible actuator-sensor configurations. Equivalent mass-spring systems were possible and were calculated for three of these configurations. WBC controllers were designed and tuned using the equivalent mass-spring systems. In each case and the closed-loop step responses were plotted.

Equivalent mass-spring representations allow quick design and tuning of WBC controllers for a much wider class of systems. Previously established analytical results concerning stability and robustness of WBC for mass-spring systems are now readily applicable to this wider class of systems. It is clear that the non-uniformity of the resulting mass-spring system and the position of this non-uniformity are key in assessing the difficulty of the control problem. From a wave based perspective large masses in the centre of the cascade lead to the trapping of waves in the outer part of the system

increasing settling times.

This paper considered only mass spring systems where the input is a force on the first mass and the output is the position of the first mass. A possible area for future research is to investigate equivalent systems where the input and output may be on different masses internal to the system. There is also scope for using similar techniques to optimise actuator and sensor locations within a system. The objective could be to make the resulting equivalent mass-spring system as close to uniform as possible.

References

[1] DODGE, F. T. the New "Dynamic Behavior of Liquids in Moving Containers". *Southwest Research Institute* (2000).

[2] GLADWELL, G. *Inverse problems in vibration*. Mechanics, dynamical systems. M. Nijhoff, 1986.

[3] KANE, T. R., AND LEVINSON, D. A. Formulation of equations of motion for complex spacecraft. *Journal of Guidance, Control, and Dynamics 3*, 2 (Mar. 1980), 99–112.

[4] O'CONNOR, W., AND LANG, D. Position Control of Flexible Robot Arms Using Mechanical Waves. *Journal of Dynamic Systems, Measurement, and Control 120*, 3 (1998), 334.

[5] O'CONNOR, W. J. A Gantry Crane Problem Solved. *Journal of Dynamic Systems, Measurement, and Control 125*, 4 (2003), 569.

[6] O'CONNOR, W. J. Excellent control of flexible systems. *Control* (2005), 6181–6186.

[7] O'CONNOR, W. J. Wave-like modelling of cascaded, lumped, flexible systems with an arbitrarily moving boundary. *Journal of Sound and Vibration 330*, 13 (2011), 3070–3083.

[8] O'CONNOR, W. J., AND FUMAGALLI, A. Refined Wave-Based Control Applied to Nonlinear, Bending, and Slewing Flexible Systems. *Journal of Applied Mechanics 76*, 4 (2009), 041005.

[9] PEREZ, E. *Vega User's Manual, Issue 3, Revision 0*. 2006.

[10] REYHANOGLU, M. Modeling and Control of Space Vehicles with Fuel Slosh Dynamics.